ELSEVIER

Materials Science and Engineering B47 (1997) 33–40

MATERIALS SCIENCE & ENGINEERING B

Chemical and microstructural properties of TiO_2 synthesized by sol-gel procedure

S. Musić *, M. Gotić, M. Ivanda, S. Popović, A. Turković, R. Trojko, A. Sekulić, K. Furić

Ruder Bošković Institute, P.O. Box 1016, 10001 Zagreb, Croatia

Received 20 September 1996; accepted 6 December 1996

Abstract

Nanosized TiO_2 powders were prepared using the sol-gel procedure. The selected colloidal suspensions were stabilized with polyethylene glycol (PEG). This polymer prevented sintering of TiO_2 particles during the calcination of the starting material. X-ray powder diffraction (XRD) phase analysis showed that the samples, obtained up to 500°C, were a mixture of anatase and brookite. In the samples, obtained at 850°C and higher temperatures, rutile as a single phase was detected. The TGA/DTA curves were dependent on the preparation of TiO_2 samples. The samples were also characterized by Fourier transform infrared spectroscopy and laser Raman spectroscopy. A new method, based on low-frequency Raman scattering, was proposed for the size determination of nanosized TiO_2. The size determination of nanosized TiO_2 by low-frequency Raman scattering was in a good agreement with crystallite size values obtained by XRD. © 1997 Elsevier Science S.A.

Keywords: Nanosized TiO_2; Sol-gel; X-ray powder diffraction; TGA/DTA; FT-IR; Low-frequency Raman scattering

1. Introduction

Titanium dioxide, TiO_2, is traditionally used as white pigment. It is used in a wide assortment of products, including paints, plastics, inks, paper, cosmetics, foodstuffs, pharmaceuticals, etc. [1]. TiO_2 also found important application as a catalyst support.

In recent years, researchers and engineers paid special attention to nanosized TiO_2, which can be utilized as dye-sensitized photoanode in a new type of solar cell as described by O'Regan and Grätzel [2] and discussed by Mallouk [3]. The mechanism of the conversion of light into electricity in this solar cell was discussed in other papers by Grätzel et al. [4–6]. Kavan et al. [7] investigated the formation of TiO_2 films on SnO_2 (F-doped) and metallic (Pt, Au and Ti) electrodes by anodic oxidative hydrolysis of acidic aqueous $TiCl_3$ solutions. Thin TiO_2 films were spectrally sensitized to higher wavelengths by adsorption of $RuL_2(\mu(NC)-Ru(CN)(bpy)_2)_2$, L = 2,2-bipyridine-4,4′-dicarboxylic acid, bpy = 2,2′-bipyridine.

Specific applications of TiO_2 are determined by the chemical, structural and physical properties of TiO_2 particles. These properties can be modified by the experimental procedure used in TiO_2 synthesis.

Vallet-Regi et al. [8] precipitated $Ti(OH)_4$ using the reaction

$$TiCl_4 + 4NH_4OH \rightarrow Ti(OH)_4 + 4NH_4Cl \quad (1)$$

The reaction products were crystalline aggregates (20–30 μm). On the other hand, pyrolysis [8,9] of aerosol droplets containing Ti(IV)-citrate yielded hollow spherical particles (1–2 μm). In dependence on the temperature of pyrolysis, up to 900°C, an amorphous fraction, brookite, anatase or rutile were formed.

A continuos production of monodispersed TiO_2 powders was developed [10]. A solution containing titanium tetraethoxide, hydroxypropylcellulose and ethanol was mixed with water-ethanol solution and the hydrolytic product was aged by continuous flow through a 100 m long Teflon tube. The particle size could be controlled between 0.2 and 0.4 μm. A minimum aging period of 10 min was required to produce monodispersed TiO_2 particles. Ikemoto et al. [11] prepared spherical and monodispersed TiO_2 particles in ethanol by mixing 0.1

* Corresponding author.

PII S0921-5107(96)02041-2

M $Ti(OC_2H_5)_4$ with 0.3 M H_2O. The TiO_2 particles were amorphous and grew up to 0.7 μm after ~10 min of hydrolysis at room temperature. Chhor et al. [12] investigated the influence of experimental procedure on the microstructure of TiO_2. TiO_2 powders were obtained from Ti(IV)-isopropoxide via three different routes, (i) thermal decomposition of titanium alkoxide in vapour phase, (ii) decomposition of titanium isopropoxide in supercritical ethanol and (iii) standard procedure of hydrolysis of Ti(IV)-isopropoxide dissolved in ethanol. Kamiya et al. [13] investigated the conditions of the production of TiO_2 fibres by hydrolysis and polycondensation of Ti(IV)-isopropoxide. In order to produce fibres by the sol-gel procedure, the conditions for the formation of primarily chain-like or linear metaloxane polymers in solutions through hydrolysis and polycondensation reactions must be carefully adjusted. This means that the initial molar ratio between Ti-alkoxide and H_2O is a very important factor in the production of TiO_2 fibres.

The correlation between the TiO_2 structure and the parameters of sol-gel synthesis (hydrolysis catalyst, pH and calcination temperature) were studied [14]. Very acidic and basic catalysts favoured the formation of rutile after thermal treatment of the TiO_2 precursor. It was found that the reaction pH did not alter either the shape or the size of the particles. An exception was observed during TiO_2 preparation in the presence of oxalic acid. Kallala et al. [15] studied the effect of H^+ ions on the growth of titanium oxopolymers. The authors measured the final structure of the polymers in gels produced under different reaction conditions according to: (i) the hydrolysis ratio which determines the potential functionality of monomers; (ii) the inhibition ratio which selects the relative rates of different reactions; and (iii) the monomer concentration, which determines how large the polymers can grow before their intergrowth. It was proposed that the growth process consisted of two stages, i.e. a few large polymers grew first, and then they densified through a capture of unused monomers. Terabe et al. [16] investigated the effects of water and hydrochloric acid on the structure and crystallization behavior of TiO_2 precursor prepared by the sol-gel procedure. Small angle X-ray scattering (SAXS) was used [17] to examine particle aggregation during the early phase gelation in the sol-gel synthesis of TiO_2.

Fine TiO_2 particles were also prepared by hydrolysis of emulsified alkoxide droplets [18]. Individual droplets acted as 'microreactors' controlling the particle composition, size and shape. The emulsion method was also used by Lianos and Papoutsi [19,20] to prepare TiO_2 particles. Ito et al. [21] prepared transparent ultrafine titanium oxide. Positively charged $Ti(OH)_4$ sol, obtained by mixing titanyl sulfate and sodium carbonate, was coagulated by the addition of sodium dodecylbenzene sulfonate (DBS), and then the coagulated colloids were transferred into the organic solvent phase by flushing. The organic solvent was removed under reduced pressure and the solid product was thermally treated below the decomposition temperature of DBS.

Nishide and Mizukami [22] observed the effect of complexing agents on the phase composition and optical properties of TiO_2 films prepared by the sol-gel procedure. Nagpal et al. [23] prepared thin films of TiO_2 and hydroxypropylcellulose (HPC) polymer onto quartz and silicon substrates using spin-coating. The crystalline TiO_2 films remained transparent until they densified at 800°C. Thin TiO_2 films were also obtained [24] by chemical vapour deposition (CVD) on different substrates in accordance with the reaction

$$TiCl_4 + 2H_2O \rightarrow TiO_2 + 4HCl \quad (2)$$

TiO_2 is also an attractive material for the production of inorganic ultrafiltration membranes showing high thermal and chemical stability, as well as a good water permeability [25,26]. Membranes with the best properties were obtained with nanosized TiO_2 particles.

In the present work the chemical and microstructural properties of TiO_2 were investigated. The sol-gel synthesis of TiO_2 was optimized. The aim of this research was to obtain nanosized TiO_2 with improved properties, which could be useful for its application as photoanode in dye-sensitized solar cells [27], as well as in electrochromic devices.

2. Experimental

Chemicals supplied by Aldrich and Merck were used. Water was doubly distilled. The TiO_2 precursor was precipitated by hydrolysis of Ti(IV)-isopropoxide in a specially designed apparatus. The glass apparatus and the experiments were designed to prevent direct contact between air atmosphere and the reacting system. The precipitation system was mixed at 500–1000 r.p.m. The experimental conditions for the preparation of TiO_2 samples are given in Table 1. The TiO_2 suspensions were dried in Petri dishes. After removal of 'free' water the solid products were analysed as prepared, or thermally treated in a tubular oven with temperature stability of ±2°C. The conditions of the thermal treatment of sample A, obtained by hydrolysis of Ti(IV)-isopropoxide, are given in Table 2. Samples B and C, stabilized by PEG (polyethylene glycol), are denoted as D and E (Table 1).

X-ray powder diffraction (XRD) measurements were performed at room temperature using a Philips counter diffractometer (MPD 1880) with monochromatized CuKα radiation.

Differential thermal analysis was performed using an instrument produced by NETZSCH. The temperature

Table 1
Experimental conditions for the preparation of TiO_2 samples

Sample	Chemical composition of the reactants	Temperature of reaction (°C)	Time of reaction (h)	Temperature and time of aging (drying)
A	10 ml isopropanol 50 ml Ti(IV)-isopropoxide 600 ml H_2O 2 ml conc. HNO_3	80	4	Aged in flask at 80°C for 24 h and at 50°C for 6 h, dried in Petri dish at 50°C for 65 h
B	5 ml isopropanol 25 ml Ti(IV)-isopropoxide 300 ml H_2O 1 ml conc. HNO_3	20	4	Dried in Petri dish at 50°C for 66 h
C	5 ml isopropanol 25 ml Ti(IV)-isopropoxide 300 ml H_2O 1 ml conc. HNO_3	80	4	Dried in Petri dish at 50°C for 42 h
D	165 ml of suspension B mixed with 10 g PEG in 50 ml H_2O			Dried in Petri dish at 50°C for 66 h
E	165 ml of suspension C mixed with 10 g PEG in 50 ml H_2O			Dried in Petri dish at 50 oC for 42 h

was controlled by a Pt-PtRh (10%) thermocouple with a heating rate of 10°C min^{-1}.

FT-IR spectra were recorded at room temperature with a Perkin-Elmer spectrometer (model 2000). The FT-IR spectrometer was coupled to a personal computer loaded with an IR Data Manager (IRDM) program. The samples were pressed into discs using spectroscopically pure KBr.

Raman scattering experiments were performed using a standard instrumental technique. A Coherent Innova-100 laser with $\lambda = 514.5$ nm served as an excitation source and the scattered light was analyzed with a DILOR Z-24 Raman spectrometer.

3. Results and discussion

3.1. General

The hydrolysis of Ti(IV)-isopropoxide in isopropanol, after addition of water, can be described by the equation

$$Ti(OC_3H_7)_4 + xH_2O \rightarrow Ti(OH)_x(OC_3H_7)_{4-x} + xC_3H_7OH \quad (3)$$

In excess of water, $Ti(OH)_4$ precipitates completely. The $Ti(OH)_4$ aggregates can be peptized into stable colloids by acidification of the suspension with HCl or HNO_3. Adsorption of H^+ ions onto the surface of $Ti(OH)_4$ aggregates gives positive charge to colloidal particles, so that these particles can exist in stabilized state. The process of adsorption of H^+ ions onto the surface of $Ti(OH)_4$ aggregates can be written as

$$n\,Ti(OH)_4 + y\,H^+A^- \rightarrow [Ti(OH)_4]_n y\,H^+ + y\,A^- \quad (4)$$

Peptization is a temperature dependent process. The phase composition of the products of aging of the TiO_2 precursor depends on its colloidal state (polymer, sol, gel or precipitate). Additional stabilization of TiO_2 colloids can be achieved with polymers, for example HPC, PEG, etc. These polymers also prevent sintering of particles during the calcination of the TiO_2 precursor.

Table 2
Conditions of the thermal treatment of sample A produced by hydrolysis of Ti(IV)-isopropoxide

Sample	Temperature of heating (°C)	Time of heating (h)
A_1	150	2
A_2	300	2
A_3	500	2
A_4	850	2
A_5	1000	2

3.2. X-ray diffraction

The characteristic parts of XRD patterns of the TiO_2 precursor (sample A) and the solid products of its thermal treatment (samples A_1, A_2 and A_5) are shown in Fig. 1. The starting material (not calcined) and the samples obtained after heating up to 500°C were identified as a mixture of anatase, as the dominant phase, and brookite. Both phases exhibited a pronounced diffraction broadening which decreased with increasing temperature. The crystallite size of these samples was estimated using the Scherrer equation

$$D = 0.9\lambda/(\beta \cos\theta) \quad (5)$$

where λ is the X-ray wavelength, θ is the Bragg angle and β is the pure full width of the diffraction line at half of the maximum intensity. The average crystallite size increased from 6 to 9 nm with an increase of the temperature up to 300°C. It is important to note that the samples analyzed in the present work showed the existence of two phases, anatase and brookite, in the starting material; this being different from many similar investigations that considered only the conversion scheme 'hydrous oxide gel → anatase → rutile'. A mixture of anatase and brookite was also observed in the

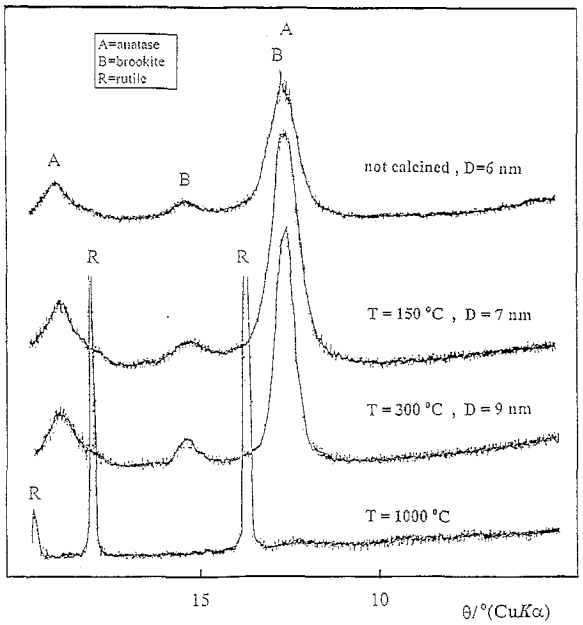

Fig. 1. Characteristic parts of the XRD powder patterns of the TiO_2 sample, denoted as A in Table 1, and of its thermal decomposition products A_1 (150°C), A_2 (300°C) and A_5 (1000°C). XRD powder patterns were recorded at room temperature. The crystallite sizes, D, are given with an estimated error of approximately 25%.

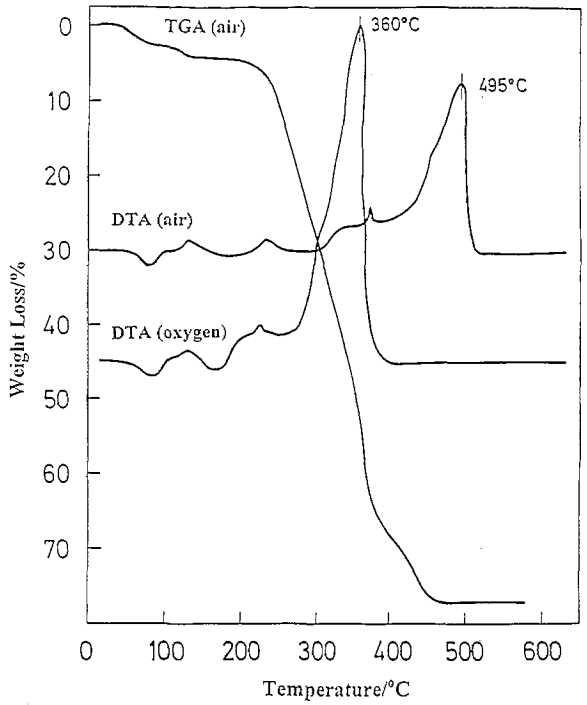

Fig. 3. TGA and DTA curves of sample D (TiO_2 stabilized with PEG). Heating rate was 10°C min^{-1}.

sample obtained after heating at 500°C. In the samples heated at 850°C and higher temperatures, rutile as a single phase was found.

3.3. Thermal analysis

Figs. 2 and 3 and 4 show the characteristic results of thermal analysis. The DTA curve of sample A (Fig. 2)

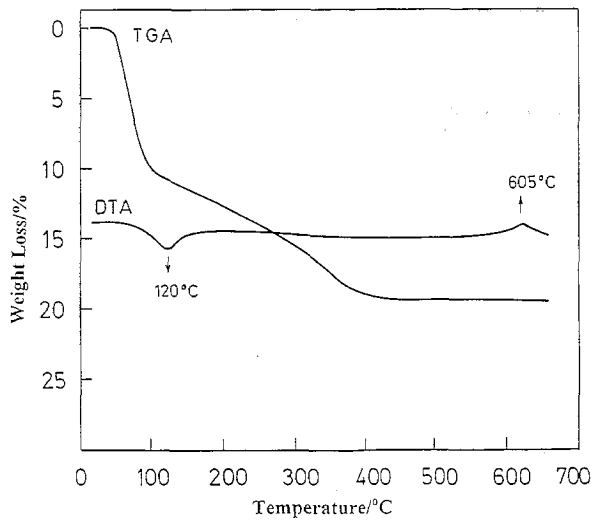

Fig. 2. TGA and DTA curves of sample A (no added PEG). Heating rate was 10°C min^{-1}.

shows an endothermic peak at 120°C due to dehydration. In Fig. 2 an exothermic peak at 605°C is also visible. Lopez at el. [14] observed a peak at 605°C during the thermal analysis of TiO_2 precursor in the presence of oxalic acid, and this peak was ascribed to the second dehydroxylation of strongly bonded OH groups. On the other hand, it was reported [28] that the transition to rutile started at 610°C, accelerated at 730°C and was completed at 915°C. Chhor at al. [12] observed a partial transition of anatase to rutile at 650°C after 4 h of heating.

The DTA curve of sample D in air (Fig. 3) shows a strong exothermic peak at 495°C due to oxidation of the organic phase. This peak is shifted to 360°C in the DTA experiment performed in an oxygen atmosphere. Similarly, the DTA curve of sample E shows oxidation peaks at 460 and 335°C, respectively (Fig. 4). The difference in the position of oxidation peaks is due to the nature of these samples. Sample B was prepared by the sol-gel procedure at 20°C, and sample C by the same procedure at 80°C. Consequently, sample B was more hydrated and showed greater interaction with PEG than sample C. Also, the degree of structural ordering was higher in sample C than in sample B. The catalytic effect of TiO_2 on the oxidation of PEG molecules was not investigated; however, this effect cannot be ruled out completely.

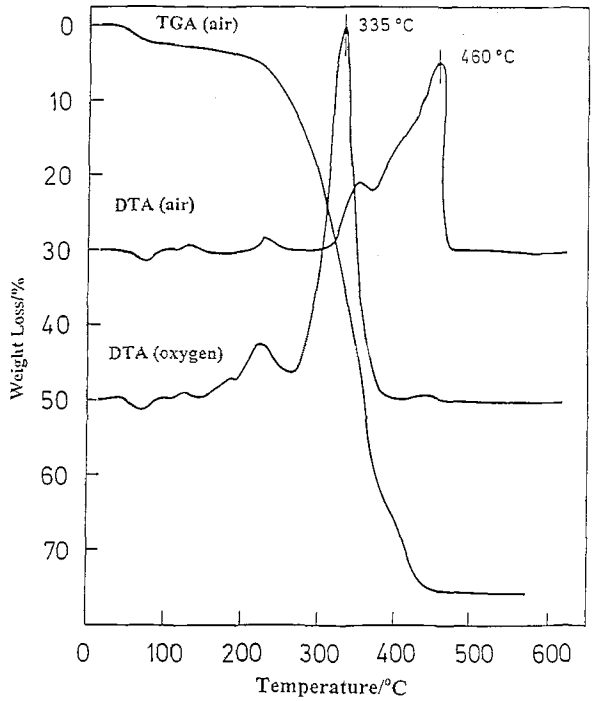

Fig. 4. TGA and DTA curves of sample E (TiO_2 stabilized with PEG). Heating rate was 10°C min^{-1}.

3.4. FT-IR spectroscopy

The results of FT-IR spectroscopic measurements are summarized in Figs. 5 and 6 and 7. The spectra of samples A, B and C showed the same spectral features (Figs. 5 and 6). The spectrum of sample A is characterized by a very strong band with two transmittance minima at 590 and 486 cm^{-1}, and a strong band at 347 cm^{-1}. Larbot et al. [29] and Chhor et al. [12] observed the same bands assigned to $\nu_{Ti\text{-}O}$ = 653-550 cm^{-1} and $\nu_{Ti\text{-}O\text{-}Ti}$ = 495–436 cm^{-1}. On the basis of the $\nu_{Ti\text{-}O\text{-}Ti}$ frequency the formation of the Ti-O-Ti bond by condensation reaction could be followed. Two OH stretching bands at 3352 and 3233 cm^{-1} are also visible. The band at 1625 cm^{-1} corresponds to the bending mode of adsorbed water. The sharp and intensive peak at 1385 cm^{-1} is due to the presence of nitrates, which were added as HNO_3 during the acidification of the system in the sol-gel synthesis. With increasing heating temperature the band at 486 cm^{-1} was shifted to 471 cm^{-1} and its relative intensity slightly increased suggesting the loss of coordinated OH groups, and consequently, the formation of new Ti-O-Ti bonds.

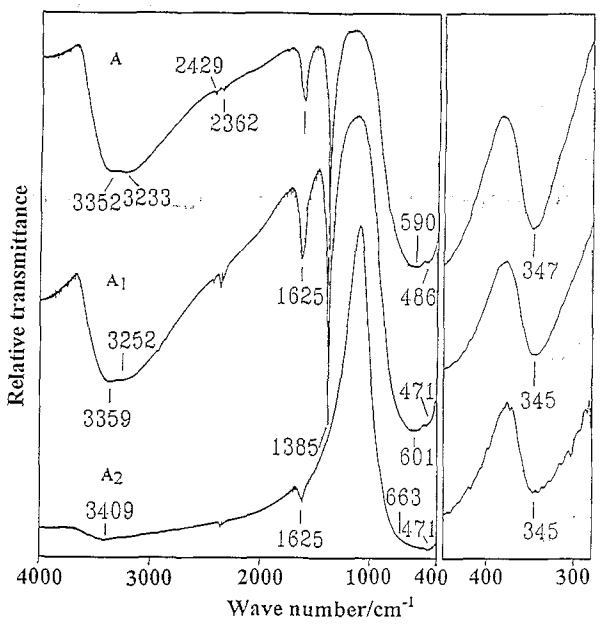

Fig. 5. Fourier transform infrared spectra of samples A, A_1 and A_2, recorded at room temperature.

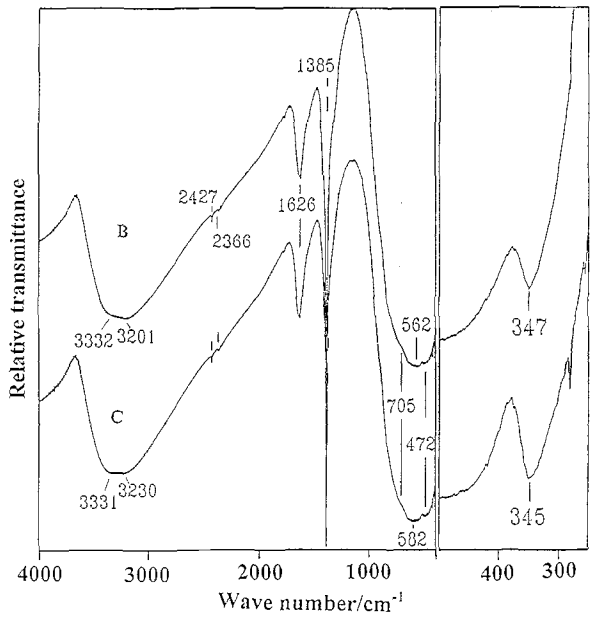

Fig. 6. Fourier transform infrared spectra of samples B and C, recorded at room temperature.

The FT-IR spectra, shown in Fig. 7, can be ascribed to rutile. Ocaña et al. [30,31] have shown that the particle shape and state of aggregation of the microcrystals have a strong effect on the IR spectrum of rutile powder.

3.5. Raman spectroscopy

In the present work, Raman spectroscopy was also used to monitor the chemical and microstructural changes in TiO_2 samples. The Raman spectra of TiO_2 polymorphs have been extensively investigated by many researchers. Before the presentation of our Raman results, some publications which appeared in this field will be shortly reviewed. For example, Tompsett et al. [32] showed that the Raman spectra of natural brookite crystals from Switzerland and Brasil and of synthetic

brookite powder are characterized by an intense band at 153 cm^{-1}. Besides several Raman bands of weak intensity, they also reported strong bands at 128 and 636 cm^{-1} and a medium intensity band at 247 cm^{-1}. Anatase shows a very strong band at 143 cm^{-1}, and rutile lacks a strong band in this region. Bersani et al. [33] observed a shift of the anatase peak from 159 to 149 cm^{-1} with an increase of the calcination temperature of the gel-derived glassy TiO_2. Felske and Plieth [34] studied the Raman spectra of electrochemically formed oxide films on Ti electrodes. They also recorded the reference spectra of anatase and rutile. The Raman spectrum of anatase powder showed characteristic bands at 645, 512, 395 and 143 cm^{-1}, while for rutile powder characteristic bands at 612, 447 and 232 cm^{-1} were recorded.

Turković et al. [35,37] investigated thermally annealed TiO_2 films. The Raman bands corresponding to anatase and rutile were assigned. Thin TiO_2 films, obtained by the spray method [36], showed a shift of the anatase peak from 143 cm^{-1} to higher wave numbers. XRD analysis of the sample indicated that the size of TiO_2 crystallites was 4.7 nm. For the sample obtained by CVD, having crystallites of size in the range of 50 nm, the most prominent band was positioned at 140 cm^{-1}. On the basis of this work, the shift of the Raman band at 143 cm^{-1} to greater wave numbers could be used as a fast probe for nanosized TiO_2. Parker and Siegel [38] explained the shift to higher wave numbers of the Raman band at 143 cm^{-1} in nanosized TiO_2 by intergrain defects due to oxygen deficiency, i.e. nanosized TiO_2 was, on an average, nonstoichiometric.

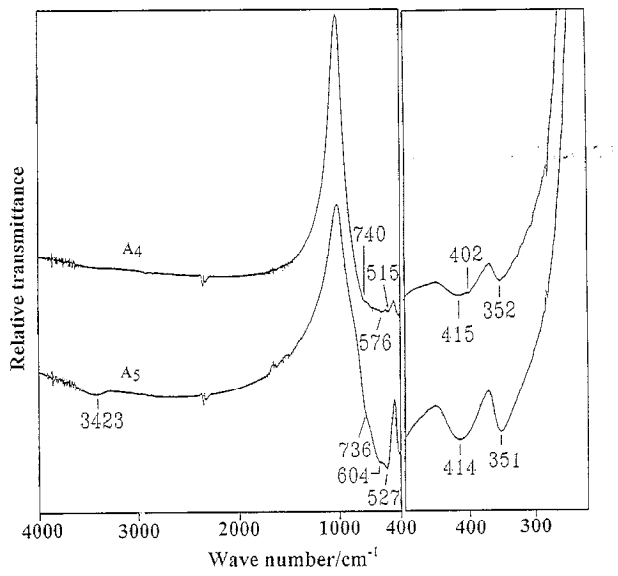

Fig. 7. Fourier transform infrared spectra of samples A_4 and A_5, recorded at room temperature.

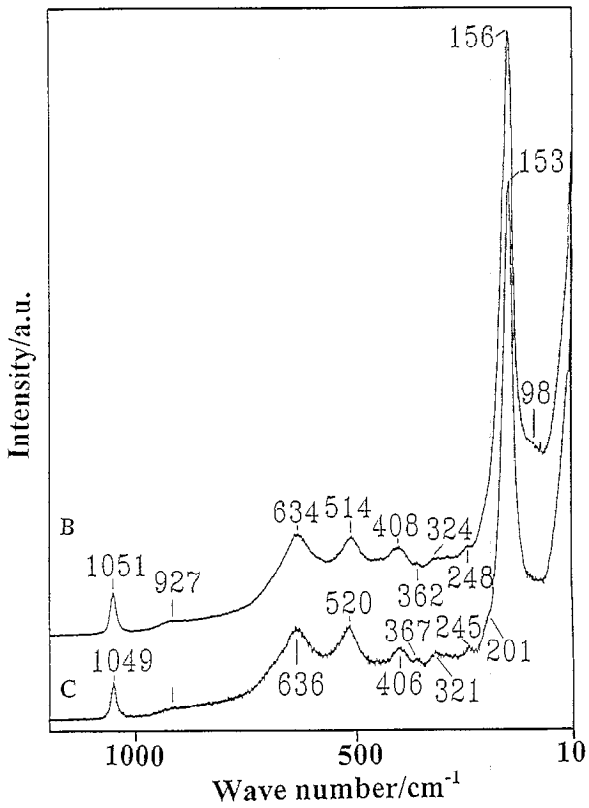

Fig. 8. Laser Raman spectra of samples B and C, recorded at room temperature.

The Raman spectra of samples A, B and C showed the same spectral features. These samples were characterized with a very strong band at 153 cm^{-1} for sample A, 156 cm^{-1} for sample B and 153 cm^{-1} for sample C. For illustration, the Raman spectra of samples B and C are shown in Fig. 8. Taking into account the literature data mentioned above, it can be concluded that the Raman spectra shown in Fig. 8 represent a mixture of anatase and brookite.

Fig. 9 shows the Raman spectra of the solid films of samples D and E, obtained by drying the colloidal suspensions of TiO_2 precursors B and C stabilized with PEG. Since these Raman spectra showed additional bands due to PEG, the reference Raman spectrum of PEG is also presented in Fig. 10. After heating sample A at 850 and 1000°C, Raman bands at 610, 447 and 238 cm^{-1} were observed. These Raman bands are typical of rutile.

In the present work we also paid attention to the size determination of nanosized TiO_2 using the method of low-frequency Raman scattering which had been tested in our previous work [39]. Generally, this method is based on the work of Duval et al. [40], originally applied to crystallized cordierite glass in the region of low-frequency Raman scattering. Duval et al. [40] showed that the maximum of the low-frequency Raman

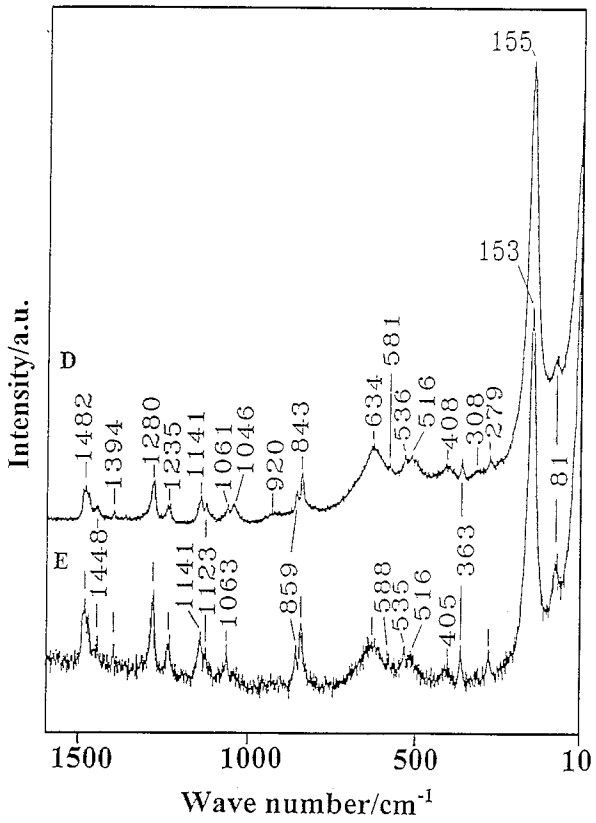

Fig. 9. Laser Raman spectra of samples D and E, recorded at room temperature.

band was proportional to the inverse diameter of the spherical spinel microcrystallites. Based on theoretical results of Lamb [41], and Tamura et al. [42], the frequency ν (in cm^{-1}) of the lowest-energy spherical mode of a free particle of spinel, corresponding to angular momentum $l = 0$, is

$$\nu \cong 0.7 v_l/(d \times c) \quad (6)$$

where c is the velocity of light in vacuum, v_l is the longitudional velocity of sound and d is particle diameter. Duval et al. [40] pointed out that the technique of Raman scattering could be a simple and good method for the characterization of nanosized particles. In addition, this method is also complementary to small angle neutron or X-ray scattering.

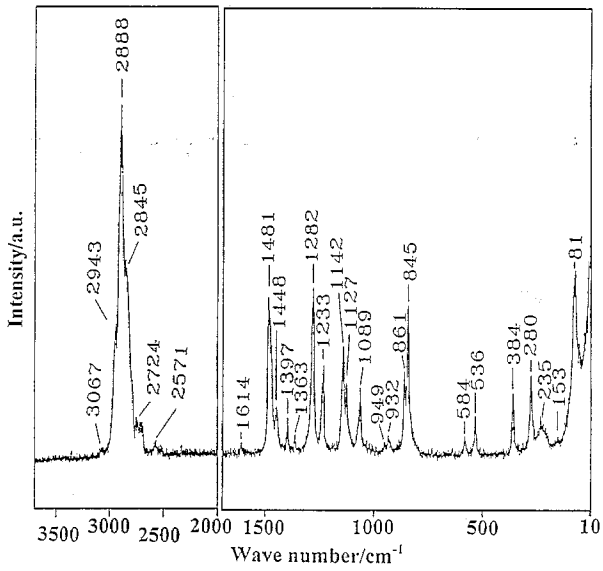

Fig. 10. Laser Raman spectrum of polyethylene glycol (PEG), recorded at room temperature.

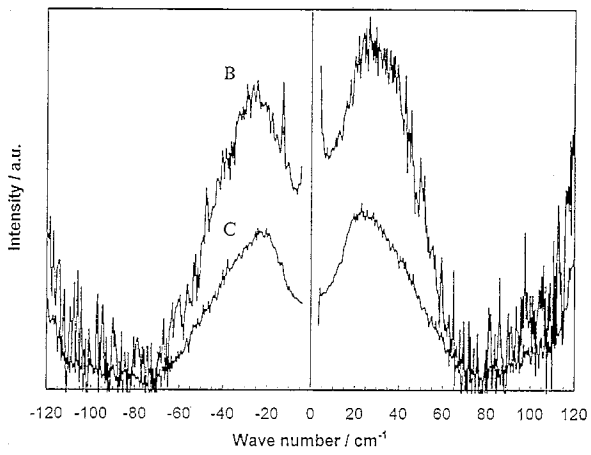

Fig. 11. Low-frequency Raman spectra, after baseline and temperature correction, of samples B and C. In the spectra the anti Stokes (−) and Stokes (+) sides are shown. The sharp peak at ≈ -13 cm^{-1} is a plasma line.

Fig. 11 shows the low-frequency Raman spectra of samples B and C. The Raman spectra were corrected supposing a linear background and according to the Bose-Einstein theory. The positions of low-frequency Raman peak, ν, and the corresponding particle diameter, d, calculated from Eq. (6) are given in Table 3. For the longitudinal velocity of sound, the average value for rutile, $v_l = 9022$ m s^{-1}, was used [43]. It is supposed that there is no great difference in the longitudinal velocity of sound in different TiO_2 polymorphs. The particle size of nanosized TiO_2 determined by low-frequency Raman scattering, as presented in Table 3, is in good agreement with crystallite size measured by XRD (Fig. 1).

Table 3
Positions of low-frequency Raman peak, ν, and TiO_2 particle diameter, d, determined from peak position

Sample	ν (cm^{-1})	d (nm)
A	30	7.0
A_1	26	8.1
A_2	21	10.0
B	29	7.3
C	24	8.8

It is known that the crystallite size does not automatically means the particle size. In previous works [44,45] we paid attention to this problem. The method of particle size determination by low-frequency Raman scattering was compared with high resolution electron microscopy (HREM). The nanocrystallite sizes were determined by X-ray diffraction and small angle X-ray scattering (SAXS). We obtained good agreement of the results obtained by these four techniques for the same samples. These works [44,45] supported our conclusion that in the present work crystallite sizes determined by XRD (in the range of estimated error) can be compared with the particle sizes determined by low-frequency Raman scattering. Also, on the basis of the present work, it can be concluded that the method by Duval et al. [40], originally developed for crystallized cordierite glass, can be also applied in particle size determination of nanosized TiO_2 and, generally, in the determination of nanosized metal oxide particles which are not inside the oxide glass matrix.

Acknowledgements

This work was supported by the Ministry of Science and Technology, Republic of Croatia (grants No. 1-07-190, 1-03-066 and 1-03-177). The authors gratefully acknowledge the support of the USA (National Institute of Standards and Technology)-Croatia (Ministry of Science and Technology) Joint Fund (grant No. JF 106). One of the authors (M.I.) would like to acknowledge the Alexander Von Humboldt fellowship.

References

[1] J.G. Balfour, in R.B. McKay (ed.), *Technological Applications of Dispersions*, Marcel Dekker, New York, 1994, p. 69.
[2] B. O'Regan, M. Grätzel, Nature 353 (1991) 737.
[3] T.E. Mallouk, Nature 353 (1991) 698.
[4] B. O'Regan, J. Moser, M. Anderson, M. Grätzel, J. Phys. Chem. 94 (1990) 8720.
[5] M.K. Nazeeruddin, P. Liska, J. Moser, N. Vlachopoulos, M. Grätzel, Helv. Chim. Acta 73 (1990) 1788.
[6] M.K. Nazeeruddin, A. Kay, I. Rodicio, R. Humphry-Baker, E. Müller, P. Liska, N. Vlachopoulos, M. Grätzel, J. Am. Chem. Soc. 115 (1993) 6382.
[7] L. Kavan, B. O'Regan, A. Kay, M. Grätzel, J. Electroanal. Chem 346 (1993) 291.
[8] M. Vallet-Regi, J. Peña, A. Martinez, J.M. González-Calbet, Solid State Ionics 63–65 (1993) 201.
[9] M. Vallet-Regi, J. Peña, A. Martinez, J.M. González-Calbet, J. Mater. Res. 8 (1993) 2336.
[10] T. Ogihara, M. Ikeda, M. Kato, N. Mizutani, J. Am. Ceram. Soc. 72 (1989) 1598.
[11] T. Ikemoto, K. Uematsu, N. Mizutani, M. Kato, Yogyo-Kyokai-Shi 93 (1985) 261.
[12] K. Chhor, J.F. Bocquet, C. Pommier, Mater. Chem. Phys 32 (1992) 249.
[13] K. Kamiya, K. Tanimoto, T. Yoko, J. Mater. Sci. Lett. 5 (1986) 402.
[14] T. Lopez, E. Sanchez, P. Bosch, Y. Meas, R. Gomez, Mater. Chem. Phys 32 (1992) 141.
[15] M. Kallala, C. Sanchez, B. Cabane, Phy. Rev. E 48 (1993) 3692.
[16] K. Terabe, K. Kato, H. Miyazaki, S. Yamaguchi, A. Imai, Y. Iguchi, J. Mater. Sci. 29 (1994) 1617.
[17] T. Kamiyama, N. Yoshida, K. Suzuki, Bull. Inst. Chem. Res., Kyoto Univ. 72 (1994) 225.
[18] A.B. Hardy, W.E. Rhine, H.K. Bowen, J. Am. Ceram. Soc. 76 (1993) 97.
[19] P. Lianos, D. Papoutsi, Progr. Coloid. Polym. Sci. 97 (1994) 240.
[20] D. Papoutsi, P. Lianos, Langmuir 11 (1995) 1.
[21] S. Ito, M. Tanaka, K. Siragane, T. Kuwahara, J. Jpn. Soc. Colour Mater. 57 (1984) 305.
[22] T. Nishide, F. Mizukami, J. Ceram. Soc. Jpn. 100 (1992) 1122.
[23] V.J. Nagpal, R.M. Davis, S.B. Desu, J. Mater. Res. 10 (1995) 3068.
[24] A. Turković, D. Šokčević, T. Valla, M. Milun, J. Rukavina, Fizika A2 (1993) 23.
[25] A. Larbot, J.P. Fabre, C. Guizard, L. Cot, J. Gillot, J. Am. Ceram. Soc. 72 (1989) 257.
[26] V.T. Zaspalis, W. Van Praag, K. Keizer, J.R.H. Ross, A.J. Burggraaf, J. Mater. Sci. 27 (1992) 1023.
[27] M. Gotić, B. Gržeta, S. Musić, S. Popović, A. Tonejc, R. Trojko and A. Turković, X-ray and Electron Diffraction, TEM, HREM and DTA of Nanosized TiO_2 as Photoanode for Dye-sensitized Solar Cell, Forth Croatian-Slovenian Crystallographic Meeting, Trakošćan, Croatia, Sept 28–30, 1995, Book of Abstracts, p. 16.
[28] D. Quin, W. Chang, J. Zhou, Y. Chen, Thermochim. Acta 236 (1994) 205.
[29] A. Larbot, I. Laaziz, J. Marignan, J.F. Quinson, J. Non-Crystall. Solids 147–148 (1992) 157.
[30] M. Ocaña, V. Fornés, J.V. Garcia Ramos, C.J. Serna, J. Solid State Chem. 75 (1988) 364.
[31] M. Ocaña, C.J. Serna, Spectrochimica Acta 47A (1991) 765.
[32] G.A. Tompsett, G.A. Bowmaker, R.P. Cooney, J.B. Metson, K.A. Rodgers, J.M. Seakins, J. Raman Spectr. 26 (1995) 57.
[33] D. Bersani, P.P. Lottici, M. Braghini, A. Montenero, Phys. Stat. Sol. (b) 170 (1992) K5.
[34] A. Felske, W.J. Plieth, Electrochim. Acta 34 (1989) 75.
[35] A. Turković, M. Ivanda, A. Drašner, V. Vraneša, M. Peršin, Thin Solid Films 198 (1991) 199.
[36] A. Turković, M. Ivanda, V. Vraneša, A. Drašner, Vacuum 43 (1992) 471.
[37] A. Turković, M. Ivanda, J. Tudorić-Ghemo, N. Godinović and I. Sorić, Oxygen Non-Stoichiometry in Thermally Annealed and Hydrogen Implanted TiO_2 Thin Films Observed by Raman Spectroscopy, in Non-Stochiometry in Semiconductors (Eds: K.J. Bachmann, H.-L. Hwang, C. Schwab) Elsevier Sci. Publ. B.V., 1992, p. 307.
[38] J.C. Parker, R.W. Siegel, J. Mater. Res. 5 (1990) 1248.
[39] M. Gotić, M. Ivanda, A. Sekulić, S. Musić, S. Popović, A. Turković, K. Furić, Mater Lett. 28 (1996) 225.
[40] E. Duval, A. Boukenter, B. Champagnon, Phys. Rev. Lett. 56 (1986) 2052.
[41] H. Lamb, Proc. London Math. Soc. 13 (1982) 187.
[42] A. Tamura, K. Higeta, T. Ichinokawa, J. Phys. C 15 (1982) 4975.
[43] M.P. Shaskolyskoii, Akusticheskii Kristal'i (in Russian), Nauka, Moscow, 1982, p. 235.
[44] A. Turković, M. Ivanda, S. Popović, A. Tonejc, M. Gotić, P. Dubček and S. Musić, Comparative Raman, XRD, HREM and SAXS studies of grain sizes in nanophase TiO_2, Proceeding of the XXIII. European Conference on the Molecular Spectroscopy, Balatonfüred, Hungary, Aug. 25–30, 1996., accepted for publication in J. Molec. Struct.
[45] A.M. Tonejc, A. Turković, M. Gotić, S. Musić, M. Vuković, R. Trojko and A. Tonejc, Mater. Lett., in press.